Ch 6 - MISCELLANEOUS TOPICS

H I – 21 cm line

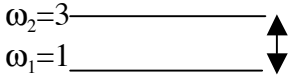

E=5.9x10-6 eV
⇒ ν=1420 MHz
⇒ λ=21.11 cm

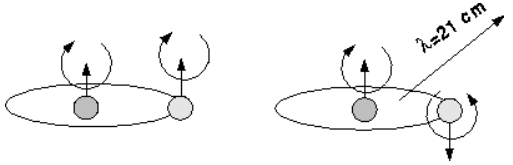

$A_{21} = 2.869 \times 10^{-15}\ s^{-1} \Rightarrow$ Lifetime $= 10^7$ years!

The transition probability is so small that the relative populations are determined by collisions, and the result is that the ratio of populations of the two states is the same as the ratio of their statistical weights = 3/1.

This line can be observed in emission or (if a suitable background source is available) in absorption.

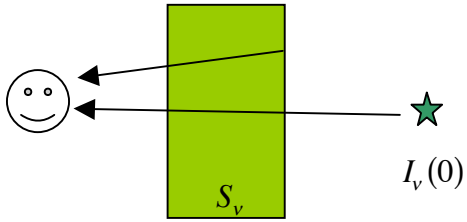

$$I_\nu = I_\nu(0)e^{-\tau_\nu} + S_\nu\left[1 - e^{-\tau_\nu}\right]$$

Rather than talk about the observed intensity, radio astronomers often use the "brightness temperature":

$$T_b = \frac{I_\nu}{\left(2k\nu^2/c^2\right)}$$

This is the temperature required for a blackbody to radiate the given intensity if one is in the Rayleigh-Jeans tail of the Planck curve – usually the case at radio wavelengths.

For no background source, in the limit that the cloud is optically thin (say $\tau_\nu << 1$) it can be shown that the column density (number of atoms along a column of cross-sectional area 1 cm^2) is

$$N(HI) = 1.82x10^{13} \int T_b(v)dv \quad atoms\ cm^{-2}$$

The situation is a little more complicated at higher optical depths.

The net result of studying the H I gas in the ISM this way (these divisions are somewhat arbitrary, but still illustrative):

"clouds"

$$\tau_{v_0} > 0.2, \quad T \sim 80\ K, \quad n_{HI} \sim 4\ cm^{-3}, \quad r \sim 15\ pc, \quad N(HI) \sim 2x10^{20}\ cm^{-2}, \quad M \sim 2x10^3\ M_\odot$$

"*cloudlets"*

$$\tau_{v_0} < 0.2, \quad T \sim 100 - 300\ K, \quad n_{HI} \sim 2\ cm^{-3}, \quad r \sim 3\ pc, \quad N(HI) \sim 2x10^{19}\ cm^{-2}, \quad M \sim 8\ M_\odot$$

"*intercloud medium"* $\left.\begin{cases} T \sim 500\ K & "warm" \\ T > 1000\ K & "hot" \end{cases}\right\} n_{HI} \sim 0.2\ cm^{-3}$

Atomic Gas Depletions

By observing lines of sites to hot stars, it is possible to measure the column densities of a variety of elements, and compare them to the abundances in the Sun. Many species are found to be depleted with respect to their solar abundances, normalized to the abundance of H.

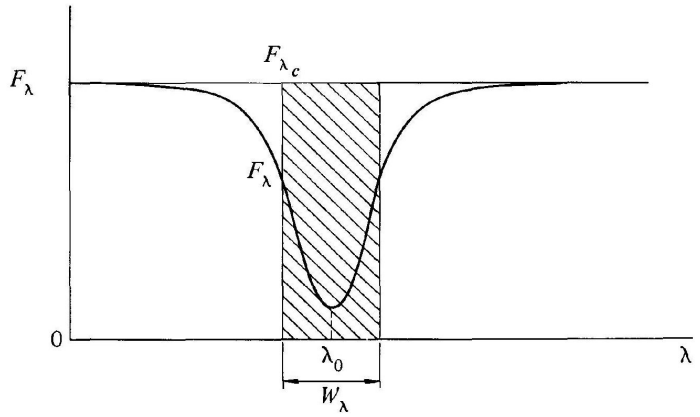

Fig. 5-7 The Equivalent Width of a Line. The equivalent width W_λ is the width of the rectangular profile for which the height is F_{λ_c} and the area is that of the spectral line. (I_λ may also be used to define the equivalent width.)

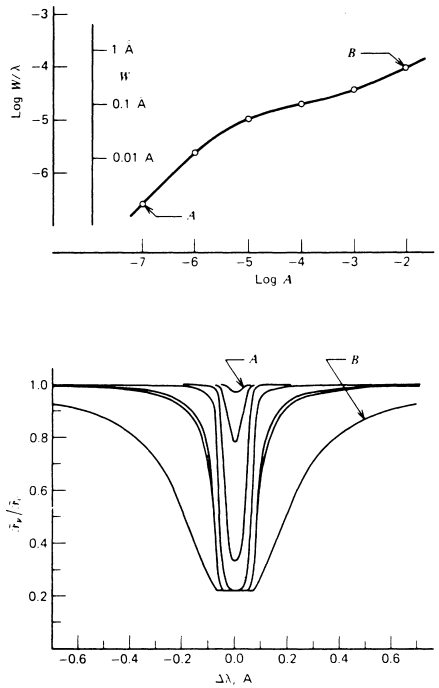

Fig. 13-12 The line strength dependence on chemical abundance of the absorbing species is shown. At the bottom the increasing profile strength is illustrated for decade steps in abundance. At the top is the curve of growth for this same line. The dots on the curve of growth correspond to the profiles below. (Computations based on a model with $S_0 = 0.87$ and $g = 10^4$.)

$$Depletion\ \delta(x) \equiv \left[\frac{\sum_{i}^{all\ ions} N(x_i)}{N(HI)+N(H_2)}\right] \Big/ \left[\frac{N(x)}{N(H)}\right]_\odot$$

$\delta(x) = 1$ for solar abundance in the gas phase.

Example: line of sight to ς Oph:

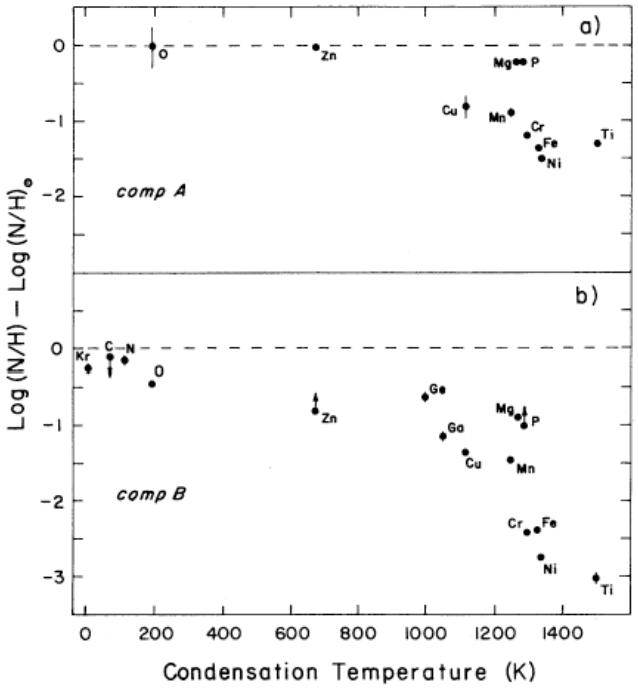

FIG. 11.—(*a*) ζ Oph logarithmic gas phase depletion, log $(N/H) - \log (N/H)_{\odot}$, for the absorption blends centered near −27 (comp A) plotted against the element's condensation temperature. The depletions in comp A are probably mostly determined by the processes that occur in cool stellar atmospheres and circumstellar environments that create the "base depletion" observed in the low-density ISM. (*b*) Same as (*a*) except for the principal ζ Oph absorption blend centered near −15 km s^{-1} (comp B). The depletions in comp B will likely be influenced by the values of "base depletion" and also by the gas phase accretion processes that likely occur in denser diffuse clouds.

From Savage et al. 1992, ApJ 401, 706.

Element	**T_c(K)**	**δ**
C,N,O	10-200	1 to 0.2
S,Zn	700	~0.7
Na,K	1000	~0.1
Si,Mg,Fe	1400	~0.03
Ti,Ca,Al	1700	~0.001

Where did these elements go? Into the formation of dust grains! In some cases, they condensed directly from the material flowing out of evolved stars, while additional depletion occurred in interstellar space. The depletions are greater when the gas is colder.

Although the depletions of C and O are not that large, their very large cosmic abundance indicates that they make up most of the mass of the grains.

For many years there was a great puzzle facing astronomers: what ARE the cosmic abundances from which these species condense from to make dust grains? Young spectral class B stars being born today seemed to have abundances of C and O that are less than our Sun. These are presumably forming from the same gas we are measuring the depletions in. So if you start off with lower abundances (those imprinted on the B stars when they formed) there is less to condense into grains. If the cosmic abundances are too low, there simply isn't enough C and O to make the grains that we see!

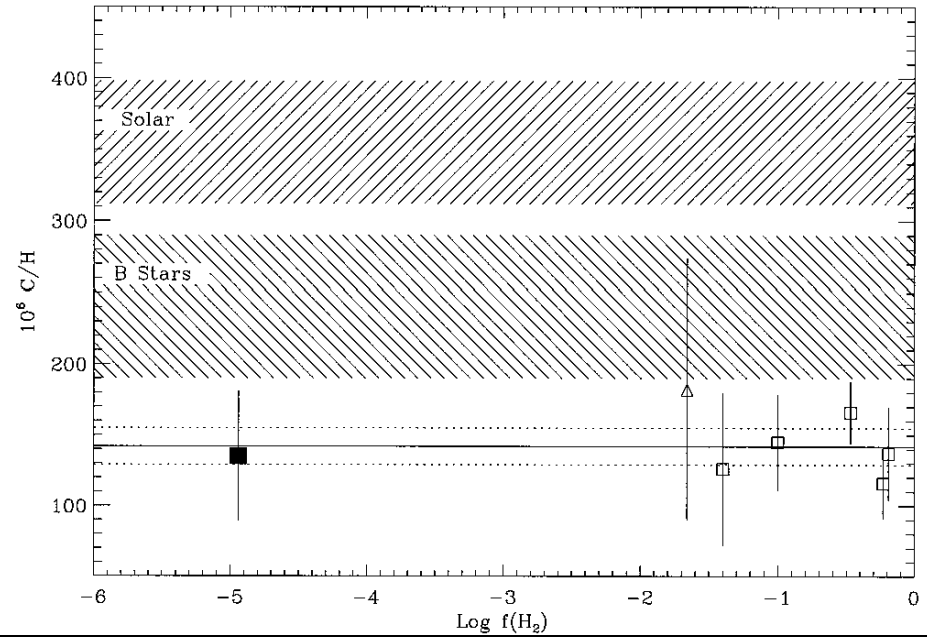

This is an example of the "B star problem" of cosmic abundances and element depletion from the interstellar gas into interstellar grains. Here the solar abundance of C (upper shaded region) was larger than that seen in young B stars being born "today" (lower shaded region). The depletion from 7 lines of sight in the interstellar medium are shown as square symbols. The further the square symbols are from the shaded regions, the greater the depletions. If the depletions are too small, there is a "budget" problem – there may not be enough depletion to account for the amount of dust we actually observe.
From Sofia et al. 1997, ApJ, 482, L105.

During the past decade, the solar abundances of both C and O have been revised downward. Affects a lot of things, including the Standard Solar Model!

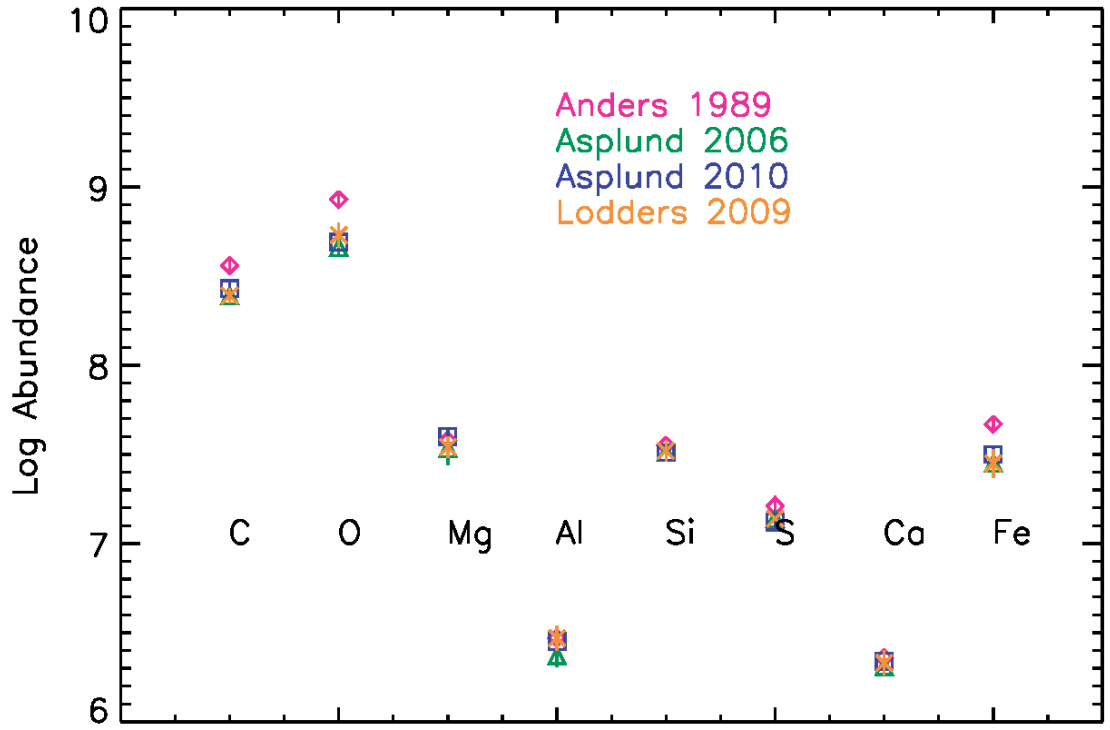

Solar abundances of the elements, from three recent sources (where the log of the abundance of H is 12.00). The solar abundances of C and O have been lowered by 20%-40% compared to the review by Anders (1989), which was the "gold standard" for many years. That brings them more in line with the B stars.

Formation of H_2

1. $H + H \rightarrow H_2 + h\nu$ Rate ~ 10^{-27}/collision! VERY RARE because it has no dipole moment and low Frank-Condon (energy overlap) factor.

2. Formation on grains

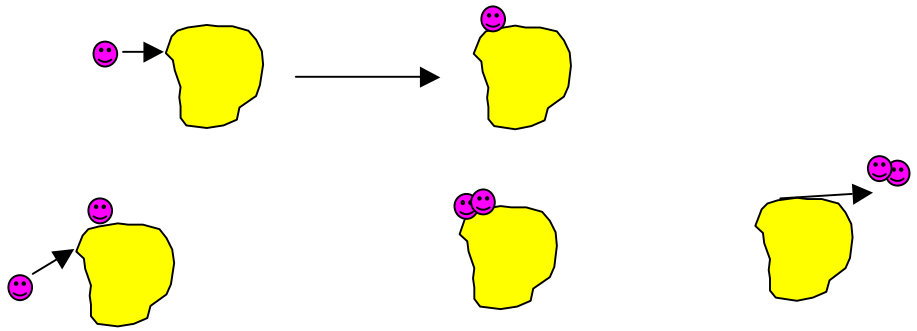

Formation Rate of H_2 on Grains

$$Rate = \underbrace{\frac{1}{2}}_{1\,H_2\ for\ 2\,H's} \left\langle \overbrace{\gamma}^{sticking\ factor} \quad \underbrace{v_{HI}\sigma_g}_{vol.swept\ out} \right\rangle \overbrace{n_g}^{\#\ grains/vol} \quad n_{HI}$$

H_2 Destruction

$$H_2 + h\nu \rightarrow H + H \quad \lambda < 850\ \mathring{A}$$

$$H_2 + h\nu \rightarrow H_2^+ + e \quad \lambda < 800\ \mathring{A}$$

$$H_2\left(X^1\textstyle\sum_g^+\right) + h\nu \rightarrow H_2\left(B^1\textstyle\sum_u^+\right) \rightarrow \begin{cases} H + H & 10\% \\ H_2\left(X^1\textstyle\sum_g^+\right)^* & 90\% \end{cases}$$

$$O^+ + H_2 \rightarrow OH^+ + H$$

$$CH^+ + H_2 \rightarrow CH_2^+ + H$$

$$C^+ + H_2 \rightarrow CH_2^+ + h\nu$$

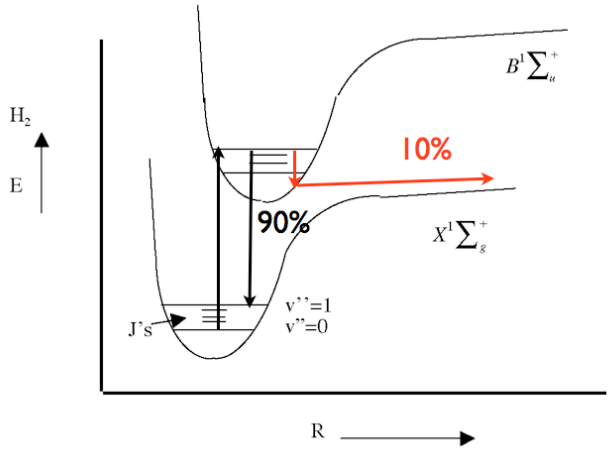

Results:

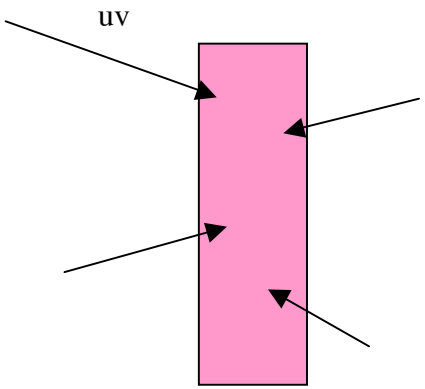

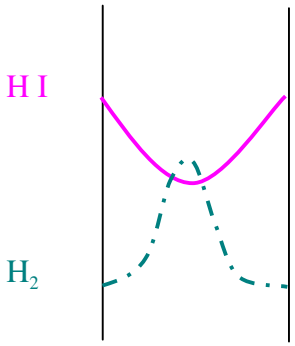

THE HOT GAS

A. Diffuse Soft X-rays 0.1-1 keV $\Rightarrow$ Thermal spectrum with T~10^6 K

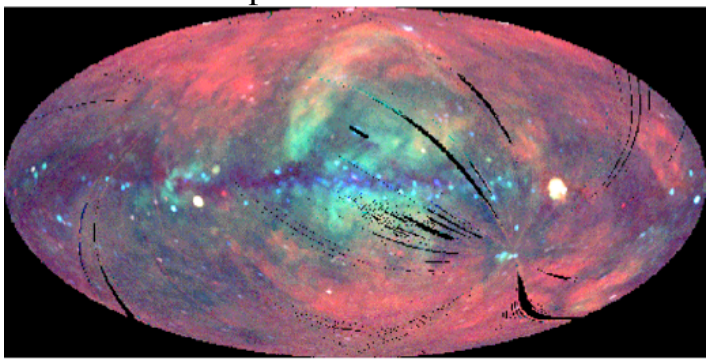

B. Interstellar O VI (O^{+5}) absorption lines at 1031 & 1038 Å

T < $2x10^6$ K from line widths
[O V $\rightarrow$ O VI needs 114 eV $\Rightarrow$ NOT photoionization but *collisional*

MODELS

Cox & Smith
("Swiss cheese model")

McKee & Ostriker

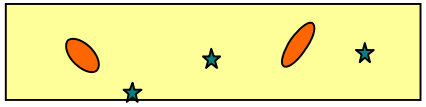

In both models, hot gas is created by heating from supernova remnants expanding outward into the interstellar medium. They differ mostly in the filling factor of the hot gas.

Local ISM

The Sun resides inside a hot bubble a few hundred parsecs in size. However, the size and shape of this region is still disputed.

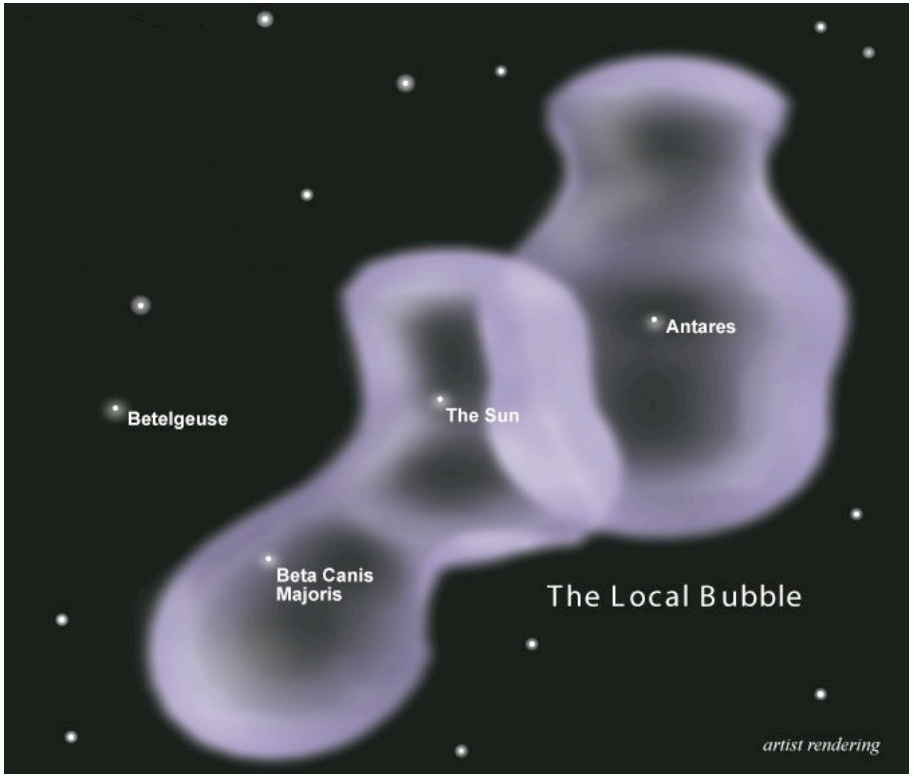

Many surveys indicate that the Sun is located in a wisp of cooler neutral gas within the hot gas region (the latter having a number density of maybe n~0.001 cm^{-3}). Here are two renditions of this local wisp.

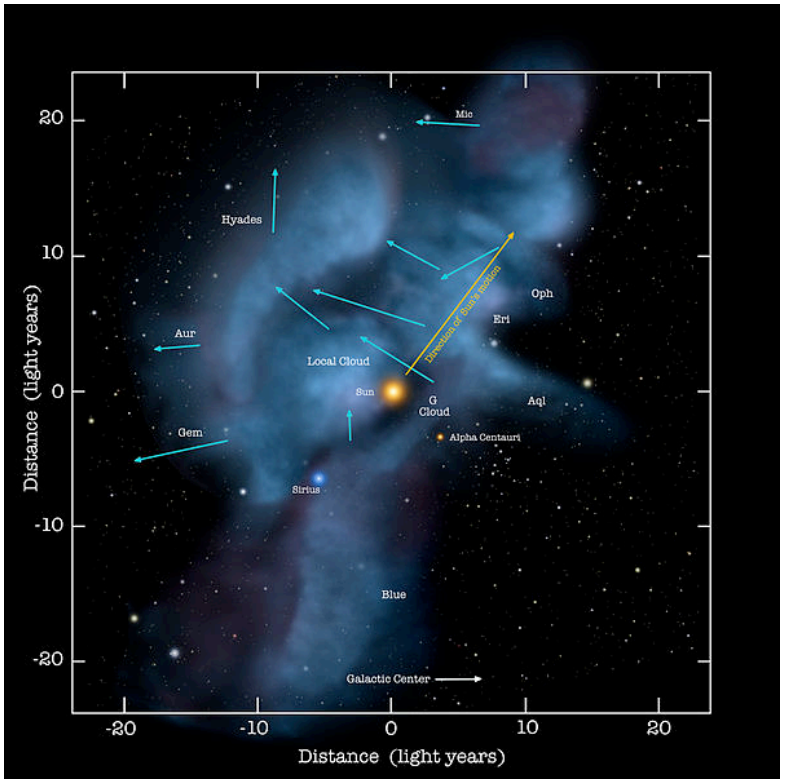

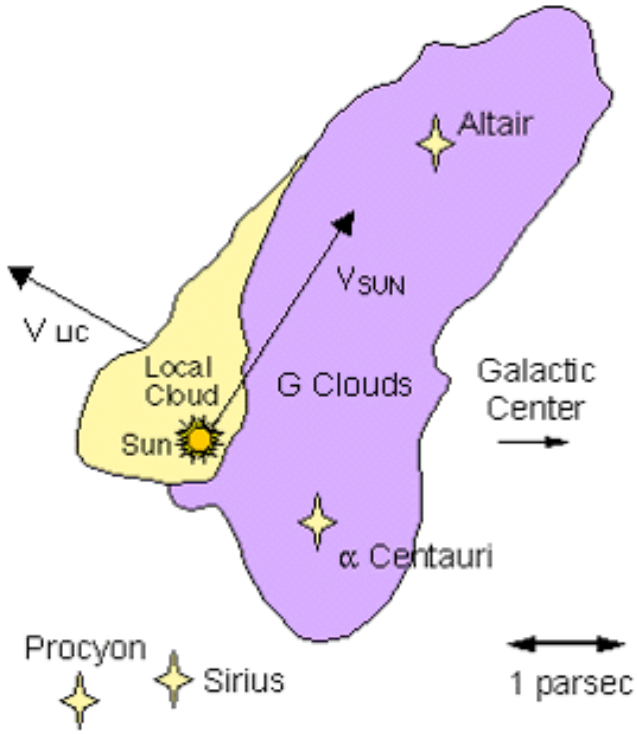

Galactic Halo Gas

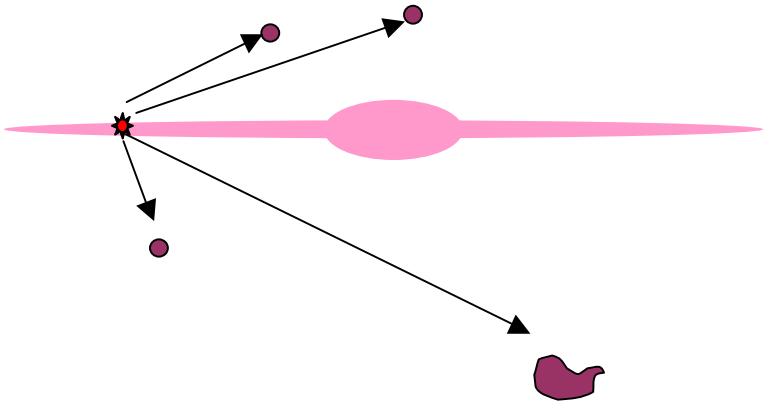

Hot stars in the halo of the galaxy, in globular clusters, and in the Magellanic Clouds, exhibit absorption lines from intervening gas. C IV, N V, and O VI are all observed at UV wavelengths (and O VII and VIII at X-ray wavelengths). Thus this "million degree" gas extends far above the galactic plane.

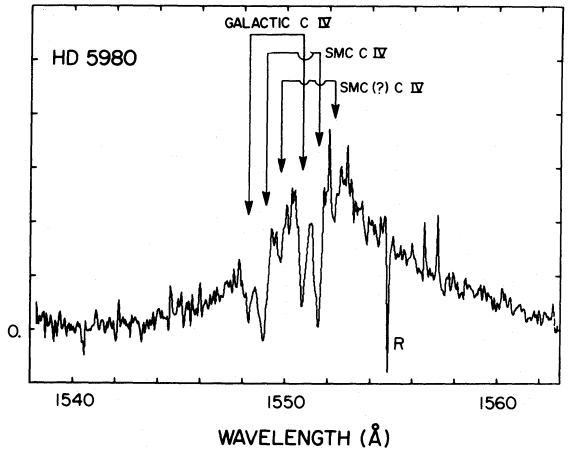

n_e of the ISM

Dependence on density, etc.:	Examples:
A. Optical or Radio Recombination Lines $\int n_e^2 d\ell$ B. Radio Free-Free Emission $\int n_e^2 d\ell$ C. Radio Free-Free Absorption $\int n_e^2 d\ell$ D. Pulsar Dispersion $\int n_e d\ell$ E. Pulsar Faraday Rotation $\int n_e \vec{B}_{\parallel} d\ell$ [and due to clumping, $\langle n_e \rangle^2 \neq \langle n_e^2 \rangle$]	**A. Diffuse galactic Hα emission** $\int I_\nu d\nu = \int \frac{1}{4\pi} h\nu_{mn} \alpha_{mn}^{eff} n_e n_{H^+} d\ell$ $\Rightarrow \langle n_e^2 \rangle \sim 0.005 - 0.015\, cm^{-6}$ **B. Radio Free-Free Emission** $j_\nu \propto n_e n_{ion} \frac{e^{-h\nu/kT}}{(kT)^{1/2}}$ **C. Radio Free-Free Absorption** $k_\nu \propto \frac{n_e n_{ion}}{T^{3/2} \nu^2}$

D. Pulsar Dispersion

Pulses propagate at the group velocity $v_g = \frac{d\omega}{dk} = c\left[1-\left(\frac{\omega_p}{\omega}\right)^2\right]^{1/2}$ $\quad Plasma\ freq.\ \omega_p = \left(\frac{4\pi n_e e^2}{m_e}\right)^{1/2}$

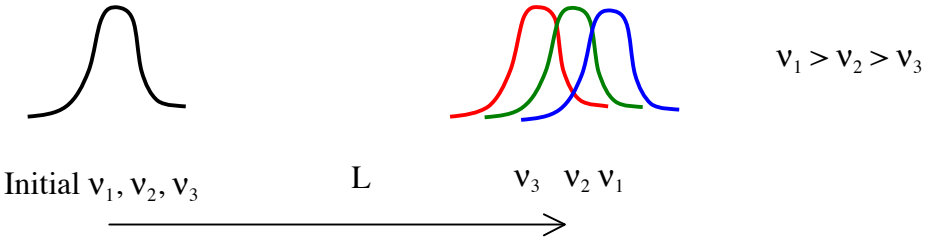

$$t = \frac{L}{v_g} = \frac{L}{c\left[1-\left(\frac{\omega_p}{\omega}\right)^2\right]^{1/2}} \approx \frac{L}{c} + \frac{L}{c}\frac{1}{2}\left(\frac{\nu_p}{\nu}\right) \qquad \nu_p = \frac{\omega_p}{2\pi}$$

$$\Rightarrow t = \frac{L}{c} + \frac{e^2}{2\pi m_e c}\frac{\langle n_e L\rangle}{\nu^2} \qquad \langle n_e L\rangle = D_m = \int_0^L n_e d\ell$$

For the Crab Nebula Pulsar,

$\Delta t_{\substack{430\ MHz \\ 111\ Mhz}} = 17.7\ s \Rightarrow \int n_e d\ell = 57\ pc\ cm^{-3}$

For some pulsars, we know L:

$\langle n_e\rangle \sim 0.03\ cm^{-3}$ in the disk of the Galaxy

$(\langle n_e\rangle^2 \approx 0.0009\ cm^{-6})$

but $\quad \langle n_e^2\rangle \approx 0.01\ cm^{-6}$

This can only be true if the ISM is clumpy.

E. Faraday Rotation

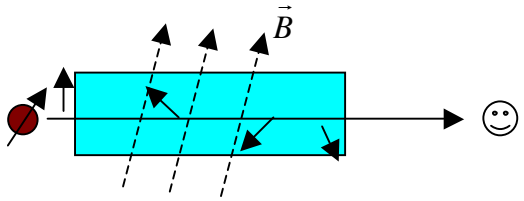

The linearly polarized signal can be decomposed into 2 circularly polarized waves. These propagate with different velocities through a magnetized plasma. The net result is to produce a phase lag between the two which manifests itself in a rotation of the orientation of the plane of polarization in the linearly polarized signal.

$$Total\ Rotation\ \Psi = R_m \lambda^2$$

$$where\ R_m = \frac{180^\circ e^3}{2\pi m_e^2 c^4} \int_0^L n_e B_\parallel d\ell$$

By combining the dispersion and Faraday rotation:

$$\Rightarrow \frac{\int_0^L n_e B_\parallel d\ell}{\int_0^L n_e d\ell} = \langle B_\parallel \rangle \sim\ few\ \mu Gauss$$

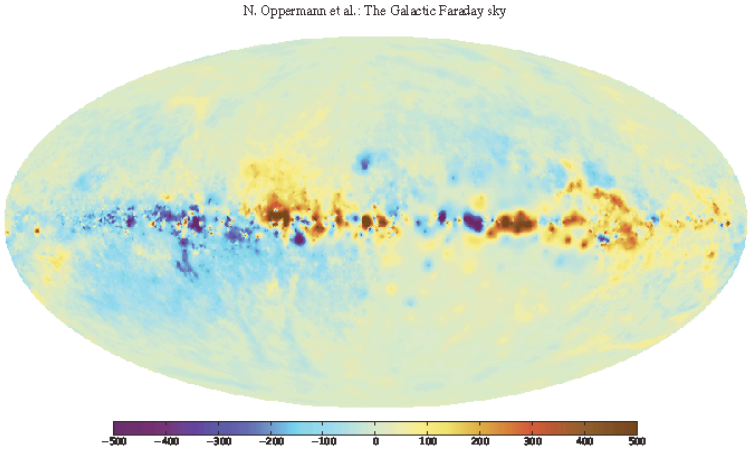

A Faraday rotation map of the sky. From Opermann et al. 2011

Galactic Synchrotron Radiation

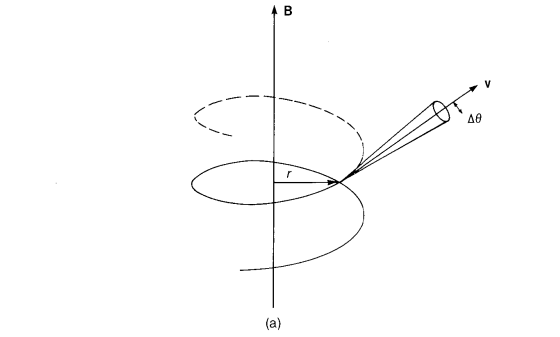

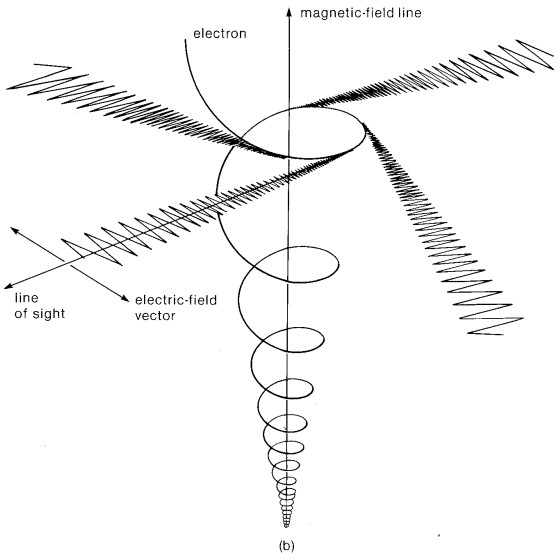

Figure 25.4. Synchrotron radiation from the electron accelerated by magnetic field: (a) angular cone containing most of the radiation; (b) polarization plane of electric field.

$$\beta = \frac{v}{c} \quad \gamma = \frac{1}{\sqrt{1-\beta^2}} \quad half-angle = \frac{1}{\gamma}$$

$$gyrofrequency\ \omega_B = \frac{eB}{\gamma mc}$$

$$Received\ Power = \frac{2}{3} r_0^2 c \gamma^2 B^2$$

Emission for a single electron with Lorentz factor γ

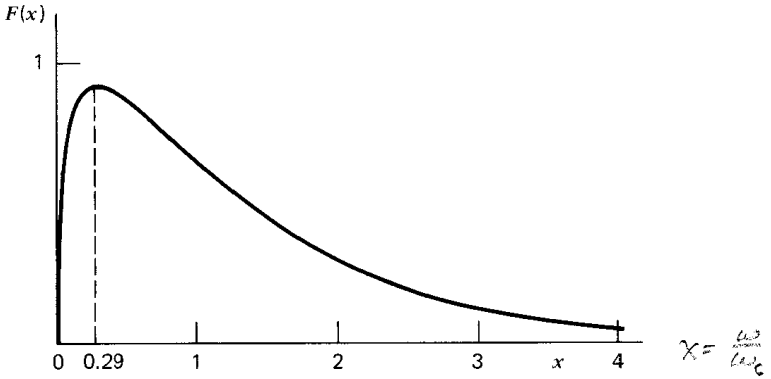

Figure 6.6 Function describing the total power spectrum of synchrotron emission. Here $x = \omega/\omega_c$. (Taken from Ginzburg, V. and Syrovatskii, S. 1965, Ann. Rev. Astron. Astrophys., 3, 297.)

$$\omega_c = \frac{3}{2}\gamma^3 \omega_B \sin\alpha \quad \alpha = pitch\ angle$$

(angle between trajectory and B filed direction)

Emergent Intensity: Emission + Absorption for a Power-Law Particle Energy Distribution $N(E) = N_0 E^{-p}$

For the galactic cosmic rays,

p ~ 2.6 for E < 5x10^{15} eV
p ~ 3.0 for E > 5x10^{15} eV

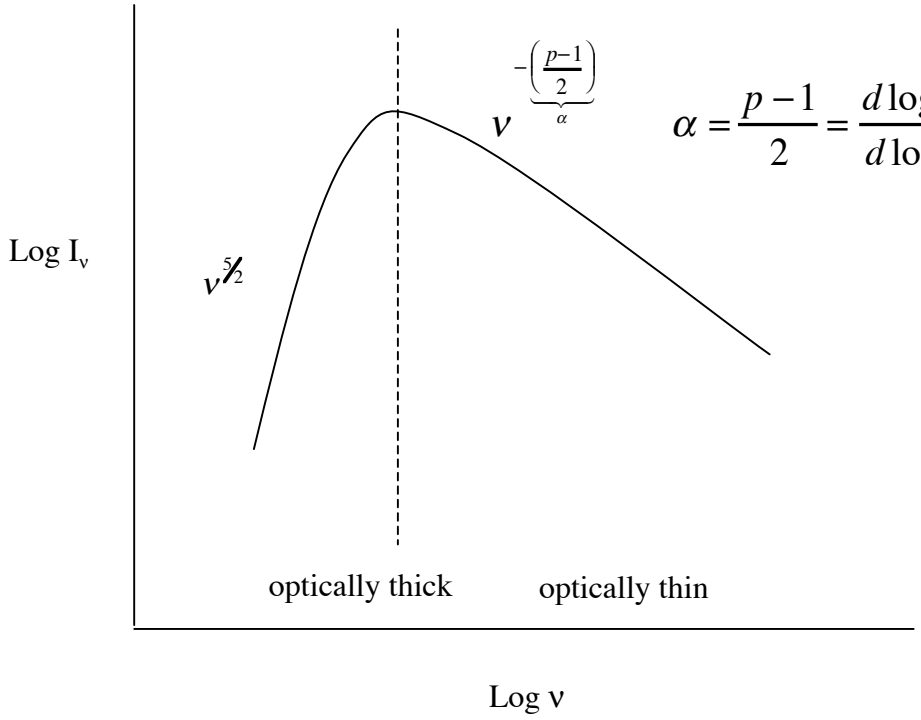

$$\alpha = \frac{p-1}{2} = \frac{d\log I_\nu}{d\log \nu} \quad I_\nu \propto \nu^{-\alpha}$$

$$\Pi_{\substack{opt \\ thin}} = \frac{p+1}{p+7/3}$$

$$\left(= 0.75 \; for \; \alpha = 1, i.e. \; p = 3\right)$$

$$\theta_{pol} \perp \vec{B}$$

$$\Pi_{\substack{opt \\ thick}} = \frac{3}{6p+13}$$

$$\left(= 0.10 \; for \; \alpha = 1, i.e. \; p = 3\right)$$

$$\theta_{pol} \parallel \vec{B}$$

Synchrotron Radiation with Energy Losses

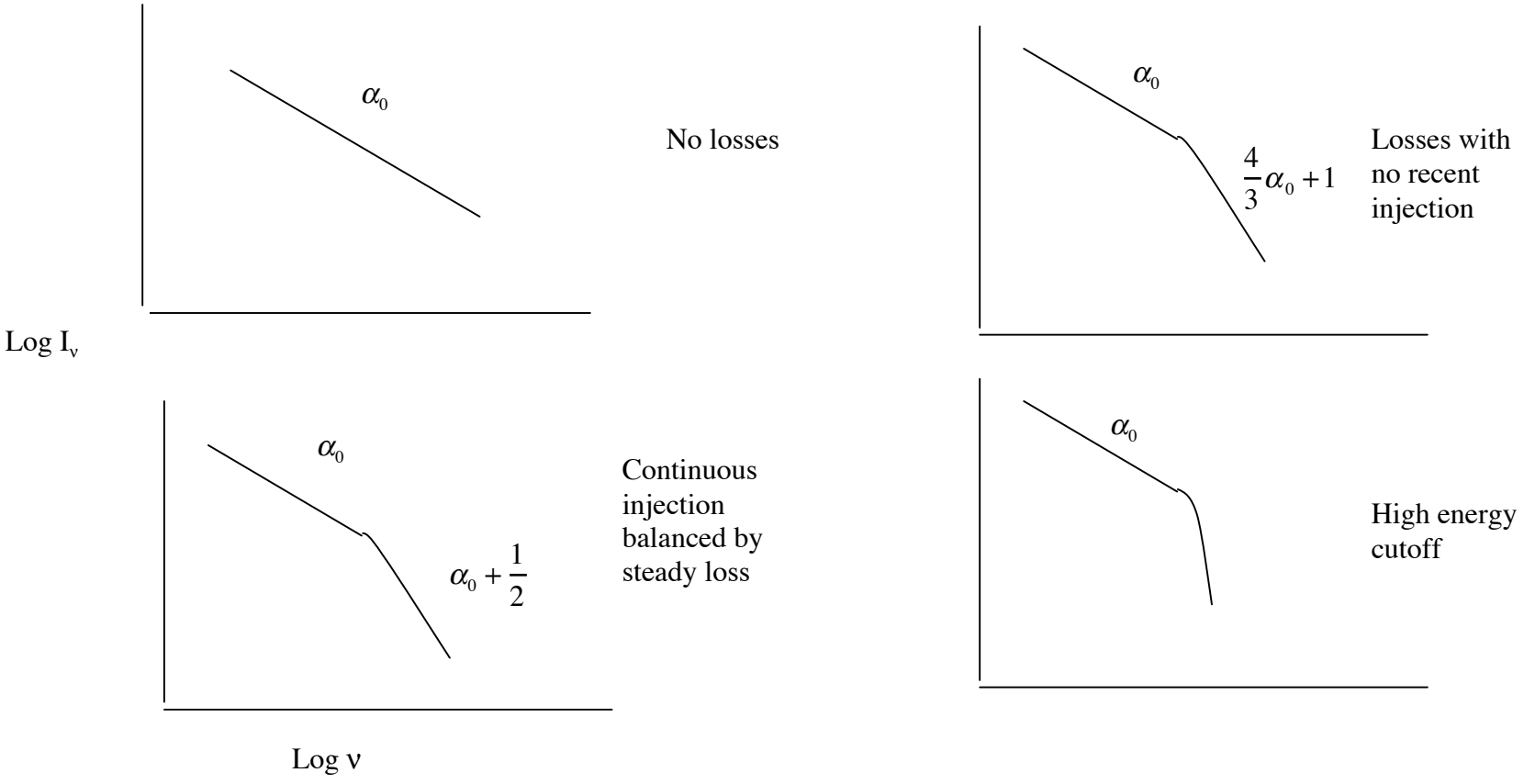

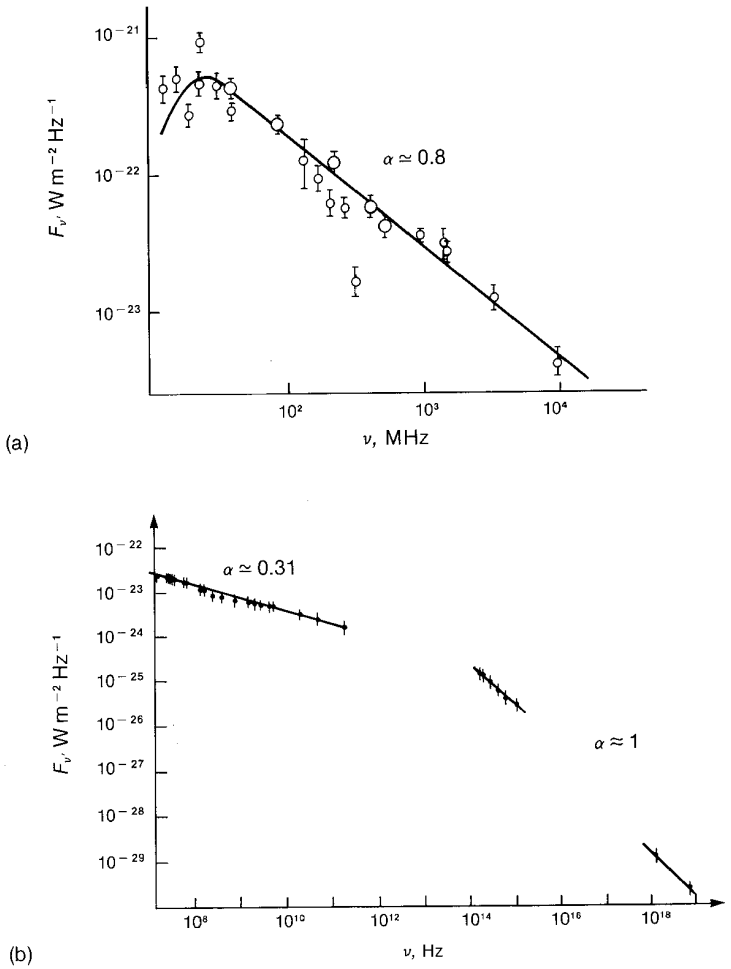

Figure 25.3. Radio spectra of two supernova remnants: (a) the Cassiopeia A nebula; and (b) the synchrotron spectrum of the Crab nebula. The spectral index and the power law α satisfy $\alpha = (\gamma - 1)/2$.